Linear Array Antenna Diagnostics Through a MUSIC Algorithm

ANGELA DELL'AVERSANO, **ANDREA NATALE**, **ANTONIO CUCCARO**,
AND RAFFAELE SOLIMENE, **(Senior Member, IEEE)**
Department of Engineering, University of Campania, Aversa 81031, Italy

Corresponding author: Raffaele Solimene (raffaele.solimene@unicampania.it)

ABSTRACT The problem of detecting defective elements in antenna arrays from near-field measurements by a MUSIC method is addressed. It is shown that, owing to the rank deficiency of the involved correlation matrix, MUSIC is indeed no better than back-transformation or matrix methods. In order to restore MUSIC performance, a rank recovering procedure is required. Therefore, here, we introduce a rank recovering method which is properly tailored to address the pertinent near-field configuration. Numerical examples, obtained for 2D scalar cases and linear array antennas, show the effectiveness of the method.

INDEX TERMS Array diagnostics, inverse imaging, multiple signal classification (MUSIC).

I. INTRODUCTION

Array antennas consist of a number of radiating elements which, depending on the applications, can sometimes be very large. Therefore, the probability that some elements are (or become) defective is not negligible. When this occurs, the array no longer works as intended. Thus, the need to find such defective elements naturally arises if some corrective strategies have to be put in place.

In order to find defective elements (array antenna diagnostics), a number of techniques have been developed, both deterministic and stochastic (see for example [1]–[6] and references therein). Here, we focus on the deterministic methods. Among them, the Back Transformation Method (BTM) is the simplest and the most commonly used [1]. Basically, this technique exploits the plane-wave spectrum representation and an FFT algorithm to back-propagate the measured field to the array aperture. Hence, this method is generally very quick but works only for planar arrays. The Matrix Method (MM) can also be applied to conformal arrays and does not require the measurements to be taken over a planar measurement aperture [7]. By this method, the discretized version of the radiation operator is inverted in order to reconstruct the radiating currents. Since the involved matrix is generally ill-conditioned, a regularization scheme must be employed [8]. While BTM has a lower computational cost, MM is more flexible and in principle can allow to achieve better performances [7]. The distributional approach presented

in [9] further generalizes MM as it does not require the element positions to be a priori known.

More recently the MUltiple SIgnal Classification (MUSIC) algorithm has been proposed for array diagnostics [10]. MUSIC is a subspace projection method borrowed from spectral estimation [11] and Degree of Arrival Estimation [12] literature. It is a super-resolving scheme but can only be used for the special case where the array defects consist of completely turned off elements [10]. However, the way MUSIC was exploited in [10] does not allow to clearly appreciate the improvement it can provide. This is because, as noted there, the involved correlation matrix is rank deficient. Consequently, MUSIC performance dramatically decreases and it actually does not work any better than BTM or MM.

The aims of this paper is twofold. First, to find an explicit connection between the MUSIC method proposed in [10] and the classical BTM and MM. This will allow to clarify the previous statement concerning the similarity of achievable performance. Second, to introduce a strategy which allows to improve the MUSIC method. As mentioned above, MUSIC performance degrades because the correlation matrix is rank deficient. Accordingly, a rank recovery step before running the MUSIC stage [13] is required. Unfortunately, for near-zone configurations, standard de-correlation methods (i.e., smoothing algorithms) cannot be directly applied. To cope with this problem, instead of working in the spatial domain, we choose to work in the spectral domain. This simple strategy permits to easily de-correlate the correlation matrix and to restore the performance of MUSIC.

The associate editor coordinating the review of this manuscript and approving it for publication was Yue Ivan Wu.

The rest of the paper is organized as follows.

In next Section we introduce the mathematical formulation. In particular, since the main aim is somehow pedagogical, we consider a simplified 2D scalar configuration and linear arrays. In this section, we also briefly recall MUSIC implementation as reported in [10] and show that, by that implementation, MUSIC is actually no better than BTM or MM. In Section 3, we describe the proposed rank recovering procedure, whereas in Section 4 some numerical examples illustrate the improvement in the achievable performances. Finally, conclusions end the paper.

II. MUSIC FOR ARRAY DIAGNOSTICS
In this section we introduce the mathematical model and the MUSIC algorithm as presented in [10]. Moreover, we compare MUSIC to an *adjoint inversion* method [14], which in turn is basically an approximation (in the sense detailed below) of MM and BTM.

A. MATHEMATICAL SETTING
Consider a 2D scalar geometry with z being the axis of invariance. Accordingly, the electric field has only the z component. Now consider a linear array of N elements arranged over the interval $SD = [-X_a, X_a]$ (where SD stands for source domain) of the x-axis. Denote as $\mathbf{r}_n = (x_n, 0)$, for $n = 1, 2, \cdots, N$, the element positions. The radiated field is observed over a rectilinear measurement aperture $MA = [-X_O, X_O]$ parallel to SD and located at distance z_O from it. Finally, denote as $\mathbf{r}_{Om} = (x_{Om}, z_O)$, $m = 1, 2, \cdots, M$, the observation points.

The corresponding radiation model is then given as

$$V(x_{Om}) = \frac{-\omega\mu}{4}\sqrt{\frac{2}{k\pi}}\exp(j\pi/4)$$
$$\times \sum_{n=1}^{N} \frac{\exp(-jk|\mathbf{r}_{Om} - \mathbf{r}_n|)}{\sqrt{|\mathbf{r}_{Om} - \mathbf{r}_n|}} h(\widehat{\mathbf{r}_{Om} - \mathbf{r}_n})$$
$$\times f(\widehat{\mathbf{r}_{Om} - \mathbf{r}_n})a_n \qquad (1)$$

where ω is the working angular frequency and k the corresponding medium wavenumber, μ the magnetic permeability of vacuum, $h(\cdot)$ and $f(\cdot)$ are the probe and the element effective heights and a_n and $V_m = V(x_{Om})$ are the excitation coefficients and the measured voltages, respectively. The array elements are assumed all equal and not interacting with each other. Moreover, in (1) each elementary radiator works in farfield. The latter is indeed a reasonable assumption since elementary radiators are much smaller than the whole array and because measurements are usually taken several wavelengths apart (so to ensure that coupling between the probe and the array under test is negligible). However, the configuration is in near-zone as far as the whole array is concerned. This is actually the model employed in [10] as well as in other papers.

In order to simplify notation, from now on we consider the unessential constant in front of the summation embodied within the coefficients a_n and cast Eq. (1) in matrix form as

$$\underline{V} = A\ \underline{a} \qquad (2)$$

where the matrix A is defined as

$$A_{mn} = \frac{\exp(-jk|\mathbf{r}_{Om} - \mathbf{r}_n|)}{\sqrt{|\mathbf{r}_{Om} - \mathbf{r}_n|}} h(\widehat{\mathbf{r}_{Om} - \mathbf{r}_n}) f(\widehat{\mathbf{r}_{Om} - \mathbf{r}_n})$$

and represents the propagator from the array to the measurement domain; the meaning of the column vectors $\underline{V}$ and $\underline{a}$ is obvious.

In order to find defective elements, and more in general to pursue the array diagnostics, eq. (2) must be solved for $\underline{a}$. In this regard, it is worth noting that the element positions enter the definition of A. Denote as $\underline{A}(\mathbf{r}_n)$ the n-th column of the propagator. Accordingly, the problem is linear, and hence "relatively" easy to solve, only when the element positions are a priori known. This is actually the framework of the MM. Nonetheless, element positions may not be precisely known. To cope with this drawback and still maintain a linear formulation, a variant of the MM method, called the distributional approach, has been introduced in [9]. By this model, actually borrowed from inverse scattering literature [15], the unknown excitations are represented as Dirac distributions whose supports are contained in SD. We leave aside details concerning what a distributional unknown formally entails as far as the mathematical framework is concerned. What matters here is that the main idea of the distributional approach is to choose a finer grid where the radiating elements can be placed. Indeed, say $N' > N$, then $2X_a/N'$ is the uncertainty at which elemental radiators can be located. In order to gain the same advantage as the distributional approach, we cast the problem under the same framework. Hence, we consider the propagator A defined as

$$A : \underline{a} \in C^{N'} \rightarrow \underline{V} \in C^M \qquad (3)$$

which of course does not mean that the number of elemental radiators has been increased. Rather, the number of radiators is still the same but their positions can be N out of N'. In principle, to reduce the uncertainty on the radiators' positions, N' could be unbounded. However, increasing N' impacts negatively on the numerical complexity and the ill-posedness of the inverse problem at hand.

According to the MM method, we consider the least square solution of (3), which is given by

$$\hat{\underline{a}} = (A^H A)^{-1} A^H \underline{V} \qquad (4)$$

where A^H is the Hermitian of A (i.e., H stands for transposition and conjugation). In order to address the ill-conditioning of A, (4) should be paired with some regularization scheme [8]. By assuming $(A^H A)^{-1} \simeq \mathcal{I}$, $\mathcal{I}$ being the identity matrix, then (4) can be approximated as

$$\hat{\underline{a}} \simeq A^H \underline{V} \qquad (5)$$

Basically, in (5) the inverse operator has been approximated by the adjoint one. This is similar to some well known

inversion schemes common in radar imaging, like migration and/or time-reversal [16]. More in detail, this inversion scheme allows to deal with the ill-posedness of the problem at hand, since it can be viewed as an inverse filtering procedure [8] where the filter is chosen according to the singular value behaviour of A. Therefore, (5) establishes a trade-off between stability and accuracy of solution, which in turn depends on the measurement aperture size. However, to be precise, it must be remarked that (5) is not a regularization scheme in the sense of Tikhonov since it does not return the generalized solution, even in absence of noise. The adjoint based inversion in (5) is also similar to the BTM. This can be understood when the Green function, and hence the propagator, is expressed in terms of the plane-wave spectrum and by noting that BTM achieves inversion by a *truncated* (because measurements are collected over a finite aperture) filtered Fourier transform, which in turn approximates the adjoint of the radiation operator.

B. MUSIC ALGORITHM

In order to perform array diagnostics, in [10] a MUSIC method has been proposed. Unlike MM, however, MUSIC method can only detect defective elements that are completely turned off. Accepting this limitation, MUSIC in principle appears a good option since it can allow for a resolution that can be much better than standard inversion schemes.

As well known, the MUSIC framework is the following. First, the so-called correlation matrix

$$R = \underline{V}\,\underline{V}^H \qquad (6)$$

is built. Then, its eigenspectrum is computed. This is done in order to separate the so-called signal, $\mathcal{S}$, and noise, $\mathcal{N}$, subspaces. In particular, if the excitation coefficients are uncorrelated, the rank of A coincides with the one of R and is N. Therefore, the data space can be factorized as $C^M = \mathcal{S} \oplus \mathcal{N}$, with $\mathcal{S} = Range(A) = span\{\underline{u}_1, \underline{u}_2, \cdots, \underline{u}_N\}$ being the range of A and $\underline{u}_n$ the eigenvectors of R. Note that in the previous discussion we have implicitly assumed that $M > N$, namely that the number of measurements is greater than the number of the elemental radiators in the array. However, it can well be that $M < N'$ since $N' > N$.

According to the data space representation, the elemental radiators that work properly correspond to the columns of A that belong to $\mathcal{S}$. Therefore, radiators' positions can be identified as the $\mathbf{r}_n$ ($n \in 1, \cdots, N'$) for which the projection of $\underline{A}(\mathbf{r}_n)$ onto $\mathcal{N}$ is zero or equivalently where the indicator

$$I(\mathbf{r}_n) = \frac{\|\underline{A}(\mathbf{r}_n)\|^2}{\|\mathcal{P}_\mathcal{N}\underline{A}(\mathbf{r}_n)\|^2} \qquad (7)$$

achieves its maxima (ideally of infinite value). In (7), $\mathcal{P}_\mathcal{N}$ denotes the projector operator onto the noise subspace and the trial column vector $\underline{A}(\mathbf{r}_n)$ (the *steering vector* in the usual MUSIC terminology) has been normalized to its Euclidean norm. Once the radiators that works correctly have been found the remaining ones are identified as being defective.

The problem of applying MUSIC in the present case is that R is singular. This is because the vector $\underline{a}$ is deterministic. Therefore, if MUSIC is applied without a rank restoring procedure (as done in [10]) then a dramatic loss in the achievable performance is experienced. Actually, the achievable performances are no better than those returned by standard BTM or MM procedures [17]. To show this, observe that for the case at hand the rank of R is just one. Accordingly, the signal subspace is the one-dimensional set $\mathcal{S} = span\{\underline{u}_1\}$ of C^M. Moreover, since $\mathcal{S} = Range(A)$, then the signal eigenvector is simply

$$\underline{u}_1 = \underline{V}/\|\underline{V}\| \qquad (8)$$

Let us rewrite (7) by using the projector operator onto the signal subspace, $\mathcal{P}_\mathcal{S} = \mathcal{I} - \mathcal{P}_\mathcal{N}$, then

$$I(\mathbf{r}_n) = \frac{\|\underline{A}(\mathbf{r}_n)\|^2}{\|(\mathcal{I} - \mathcal{P}_\mathcal{S})\underline{A}(\mathbf{r}_n)\|^2} \qquad (9)$$

with

$$\|(\mathcal{I} - \mathcal{P}_\mathcal{S})\frac{\underline{A}(\mathbf{r})}{\|\underline{A}(\mathbf{r})\|}\|^2 = 1 - |<\frac{\underline{A}(\mathbf{r})}{\|\underline{A}(\mathbf{r})\|}, \underline{u}_1 >|^2 \qquad (10)$$

and $<\underline{x}, \underline{y}> = \underline{x}^H\,\underline{y}$ is the scalar product in C^M.

From (10) and in view of (8) and (9), one deduces that it is not necessary to compute the eigenspectrum of R to build the indicator function. This fact of course is relevant from the computational point of view and seems to have been completely missed in [10]. Furthermore, the detection ability of the MUSIC is now clearly linked to the behavior of the scalar product $|<\underline{A}(\mathbf{r}_n)/\|\underline{A}(\mathbf{r}_n)\|, \underline{u}_1 >|$ which, when (8) is used, can explicitly be written as

$$<\frac{\underline{A}(\mathbf{r}_n)}{\|\underline{A}(\mathbf{r}_n)\|}, \underline{u}_1 > = \frac{\underline{A}(\mathbf{r}_n)^H\,\underline{V}}{\|\underline{A}(\mathbf{r}_n)\|\|\underline{V}\|} = \frac{\hat{a}_n}{\|\underline{A}(\mathbf{r}_n)\|\|\underline{V}\|} \qquad (11)$$

where (5) has been used in the last term on the right hand side. Accordingly, (7) can be rewritten as

$$I(\mathbf{r}_n) = \frac{(\|\underline{A}(\mathbf{r}_n)\|\|\underline{V}\|)^2}{(\|\underline{A}(\mathbf{r}_n)\|\|\underline{V}\|)^2 - (|\hat{a}_n|)^2} \qquad (12)$$

Eq. (12) is the sought after link between MUSIC and MM. It is now clear that the achievable resolution is basically related to $\hat{\underline{a}}$ and hence it is the same for both methods. In other words, if two elements are not resolved in $\hat{\underline{a}}$, MUSIC will fail to resolve them as well. Indeed, the MUSIC method presented in [10] seems to perform better than MM simply because of the use of the function in (7) (instead of the mere $|<\underline{A}(\mathbf{r}_n), \underline{u}_1 >|$) which *only* makes the MUSIC indicator sharper than the MM reconstruction in correspondence to the radiating elements.

III. RECOVERING THE RANK OF R

In order to exploit the super-resolving capability of MUSIC algorithm it is necessary to recover the rank of R, or equivalently to have the signal subspace dimension equal to the number of correctly working elements ($\leq N$). To this end, one can consider exploiting some de-correlation methods

(i.e., smoothing procedures), which have been developed to deal with coherent or partially coherent signals [18]. Unfortunately, all the smoothing procedures found in literature require the field to exhibit a special dependence on the observation variable x_{Om} and the element positions x_n. In particular, the rank recovering is simple to achieve if the operator matrix has a form like $A_{mn} = \alpha \exp(j\beta x_{Om} x_n)$, with α and β being constants. Clearly, this is not the case here (see eq. (1)). Fortunately, model (1) can be recast in a form suitable for smoothing by a simple Fourier transformation. Indeed, by rewriting (1) in the spectral domain yields

$$\hat{V}(k_x) = \frac{h(k_x)f(k_x)}{k_z} \exp(-jk_z z_O) \sum_{n=1}^{N} \exp(-jk_x x_n) a_n \quad (13)$$

where $\hat{\ }$ denotes the Fourier transform, k_x is the spectral variable and $k_z = \sqrt{k^2 - k_x^2}$ is real since evanescent waves are considered negligible. Note also that the truncation effect due to the finite measurement aperture has not been considered. To further simplify the notation, we normalize the term $h(k_x)f(k_x)/k_z \exp(-jk_z z_O)$ which is basically equivalent to performing the so-called probe and element correction. Accordingly, we have

$$\hat{V}(k_{xm}) = \sum_{n=1}^{N} \exp(-jk_{xm} x_n) a_n \quad (14)$$

where we continued to denote as $\hat{V}$ the Fourier transform of the normalized voltage. The observation variables is now $k_{xm} = m\Delta_k$, for $m = -M', \cdots, M', M' = (M-1)/2$, M is assumed odd, and Δ_k is the step in the wavenumber domain. (14) is now in the "right" form for the application of a smoothing procedure. In particular, this can be easily achieved by rearranging the data vector $\underline{\hat{V}}$ in a Toeplitz matrix as

$$Tp(\underline{\hat{V}}) = \begin{pmatrix} \hat{V}_0 & \hat{V}_1 & \cdots & \hat{V}_{M'} \\ \hat{V}_{-1} & \hat{V}_0 & \cdots & \hat{V}_{M'-1} \\ \vdots & \vdots & \ddots & \vdots \\ \hat{V}_{-M'} & \hat{V}_{-(M'-1)} & \cdots & \hat{V}_0 \end{pmatrix} \quad (15)$$

which maps $C^{M'}$ over $C^{M'}$. The rank of $Tp(\underline{\hat{V}})$ can be easily deduced once it is factorized as follows

$$Tp(\underline{\hat{V}}) = B \, diag(\underline{a}) \, B^H \quad (16)$$

where

$$B = \begin{pmatrix} 1 & 1 & \cdots & 1 \\ \zeta_1 & \zeta_2 & \cdots & \zeta_N \\ \vdots & \vdots & \vdots & \vdots \\ \zeta_1^{M'} & \zeta_2^{M'} & \cdots & \zeta_N^{M'} \end{pmatrix} \quad (17)$$

and

$$diag(\underline{a}) = \begin{pmatrix} a_1 & 0 & \cdots & 0 \\ 0 & a_2 & \cdots & 0 \\ \vdots & \vdots & \ddots & \vdots \\ 0 & 0 & \cdots & a_N \end{pmatrix} \quad (18)$$

and $\zeta_n = \exp(-j\Delta_k x_n)$. Indeed, as long as $M' > N$, since B is a Vandermonde matrix, the rank of $Tp(\hat{V})$ coincides with the number of a_n which are not zero, that is the number of elemental radiators working correctly. Hence, the rank is actually restored and at most can be N. Also, it is seen that the range of $Tp(\hat{V})$ is spanned by the columns of B. For convenience denote as $\underline{\zeta}(\mathbf{r}_n) = (1, \zeta_n, \cdots, \zeta_n^{M'})^T$, T meaning transposition. Accordingly, the element positions can be found by building an indicator function like (7) which now particularizes as

$$I(\mathbf{r}_n) = \frac{\|\underline{\zeta}(\mathbf{r}_n)\|^2}{\|\mathcal{P}_\mathcal{N}\underline{\zeta}(\mathbf{r}_n)\|^2} \quad (19)$$

Here, we continued to denote the projector onto the noise subspace as $\mathcal{P}_\mathcal{N}$, even though now such a space is $C^{M'} - Range(Tp(\hat{V}))$. Also, as opposed to the MUSIC version in [10], here, in order to implement the projector onto the noise subspace, the eigenspectrum of $Tp(\hat{V})$ must be computed.

It is remarked that after the rank recovering procedure is applied, the dimension of the noise subspace reduces. Indeed, while for uncorrelated signals the noise subspace dimension is $M - N$, for (19) it is $M' - N$. In other words, half the measurements are used to restore the rank. This reduction can impact on the achievable performances and put a more stringent limit on the size of the arrays that can be diagnosed since $N < M' = (M-1)/2$ must hold. This drawback is common to any smoothing procedure, even though it can be less severe by employing the forward-backward smoothing method [19]. However, under particular circumstances, this drawback can be avoided completely. In particular, for the case at hand, this happens if the excitation coefficients are all real. Indeed, if the a_n are all real then the data vector can be arranged as

$$Tp_r(\underline{\hat{V}}) = \begin{pmatrix} \hat{V}_{-M'} & \hat{V}_{-(M'-1)} & \cdots & \hat{V}_{M'} \\ \hat{V}_{-(M'-1)}^* & \hat{V}_{-M'} & \cdots & \hat{V}_{M'-1} \\ \vdots & \vdots & \ddots & \vdots \\ \hat{V}_{M'}^* & \hat{V}_{(M'-1)}^* & \cdots & \hat{V}_{-M'} \end{pmatrix} \quad (20)$$

where $*$ means conjugation. It is easy to verify that $Tp_r(\hat{V})$ enjoys the same factorization as $Tp(\hat{V})$ with B being replaced by

$$B_r = \begin{pmatrix} \zeta_1^{*M'} & \zeta_2^{*M'} & \cdots & \zeta_N^{*M'} \\ \vdots & \vdots & \vdots & \vdots \\ \zeta_1^* & \zeta_2^* & \cdots & \zeta_N^* \\ 1 & 1 & \cdots & 1 \\ \zeta_1 & \zeta_2 & \cdots & \zeta_N \\ \vdots & \vdots & \vdots & \vdots \\ \zeta_1^{M'} & \zeta_2^{M'} & \cdots & \zeta_N^{M'} \end{pmatrix} \quad (21)$$

Therefore, while the rank of $Tp_r(\hat{V})$ is the same as $Tp(\hat{V})$, now the noise subspace is clearly $C^M - Range(Tp_r(\hat{V}))$ and hence its dimension turns out to be $M - N$. The corresponding MUSIC indicator has the same form as (19) but the columns
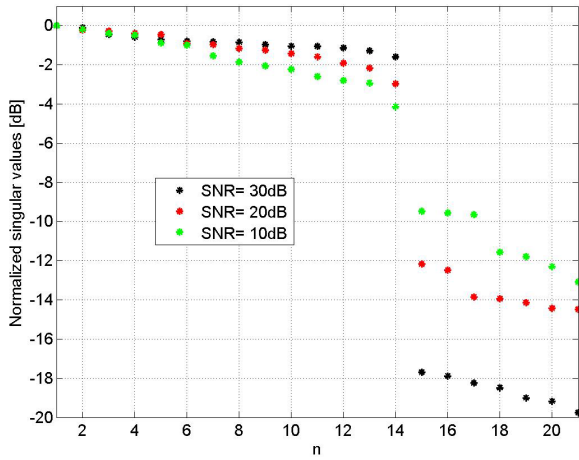
FIGURE 1. Normalized eigenvalue value behavior of $Tp_r(\hat{V})$ for different SNR.

of B_r must be used as trial vectors. For this case, in the sequel, the indicator will be denoted as I_r.

IV. NUMERICAL EXAMPLES

In this section we report some numerical examples in order to corroborate previous arguments. In particular, for the sake of simplicity, we consider the array elements as well as the probe antennas to be isotropic 2D radiators. The excitation coefficients are assumed real so that the formulation in (20) and the corresponding indicator I_r are employed. The indicator resulting from the MUSIC method presented in [10] is instead indicated as I.

As a first example we consider a slice (linear array) that mimics the array configuration addressed in [10]. In particular, the linear array consists of $N = 27$ elements arranged uniformly over $SD = [-6.5\lambda, 6.5\lambda]$, λ being the wavelength, whereas the radiated field is collected at $z_O = 5\lambda$ over the measurement aperture $[-20\lambda, 20\lambda]$ and sampled at $\lambda/2$, hence $M = 81$. The defective elements are 13 and are all located on the same side of the array. In Fig. 1, the eigenvalue behaviour of $Tp_r(\hat{V})$ is reported for different SNR whereas in Fig. 2 the corresponding indicators I_r and I are compared.

From Fig. 1 it can clearly be appreciated that the rank recovering procedure works very well. Indeed, even for a relatively high level of noise, the number of working elements is clearly determined. Moreover, the signal eigenvalues are well discerned from the noise ones. This allows to easily identify the noise subspace. This circumstance occurs also for the other examples in the following. Therefore, for such cases we omit to report the corresponding eigenvalue behavior again. As to the defective element detection, Fig. 2 shows that both methods succeed in finding them under different noise levels. However, I_r is definitely better. Indeed, the indicator amplitude range is much higher, which entails a sharper detection. Moreover, while the method in [10] fails to resolve the working elements, I_r does. This is a clear indication that the proposed method has a better resolution.

Nonetheless, as previously said, both methods identify the defective elements and hence it is natural to inquire if the proposed method is really worth using. We need hence to elaborate more in depth on this question. First, it is
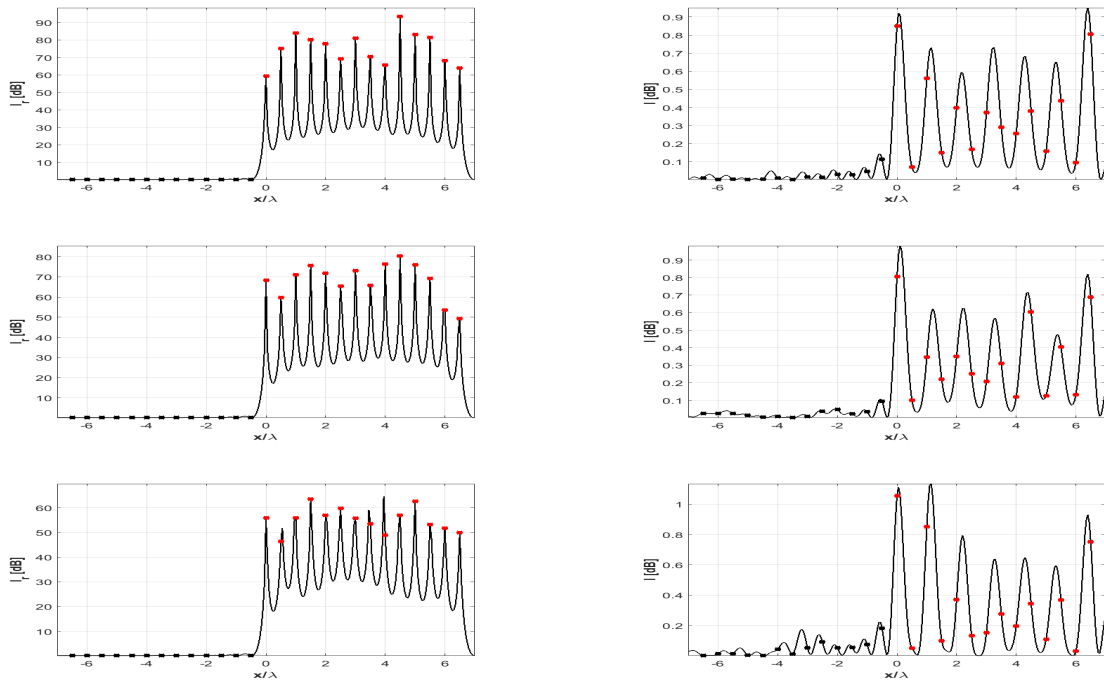
FIGURE 2. The array consists of 27 elements. The defective ones are denoted by black bullets whereas the working ones as red bullets. For (a) and (b) SNR= 30*dB*, for (c) and (d) SNR= 20*dB* and for (e) and (f) SNR= 10*dB*. Left column report I_r whereas the right one the results reported by the method described in [10].
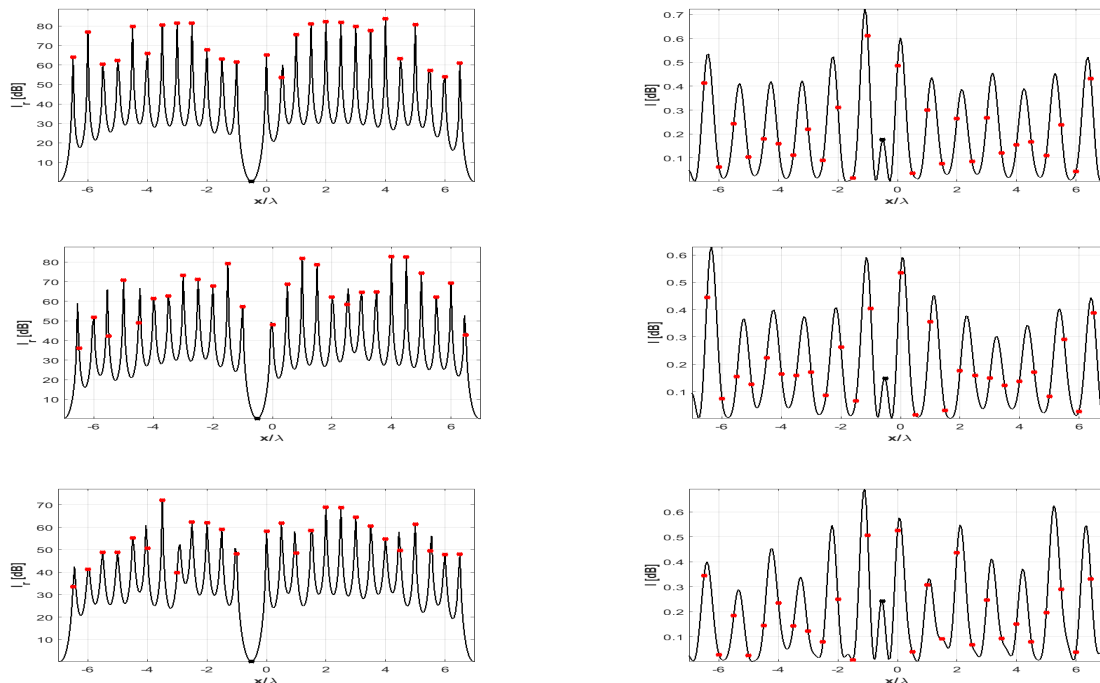
FIGURE 3. The case of a single defective element located at position 13. The configuration parameters are the same as Fig. 2. The defective element is denoted by a black bullet whereas the working ones as red bullets. For (a) and (b) SNR= 30*dB*, for (c) and (d) SNR= 20*dB* and for (e) and (f) SNR= 10*dB*. Left column report I_r whereas the right one the results reported by the method described in [10].
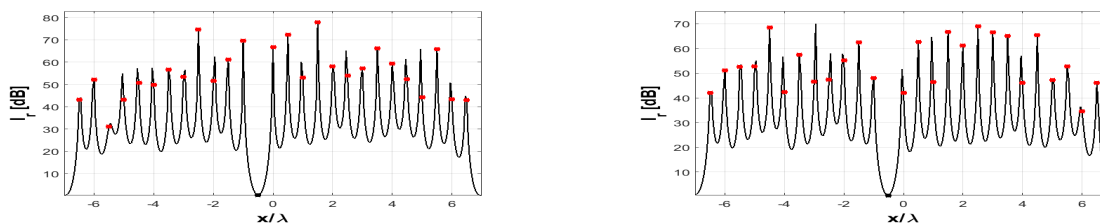
FIGURE 4. The effect of reducing the measurement aperture (*MA*). The configuration parameters are the same as Fig. 3 with *MA* = [−10λ, 10λ] in (a) and *MA* = [−7λ, 7λ] in (b). The number of measurement is 41 and 29, respectively. *SNR* has been fixed at 20*dB*.

noted that in the previous example the defective elements are close to each other and on the same side. This actually simplifies the detection stage. A more difficult scenario is when a defective element occurs amidst two that works properly. Indeed, in this case, because of the limited resolution, the reconstruction of the working elements may hide the defective one. Therefore, in order to check our method under such circumstances, we chose to consider the extreme case whereby only one non-functional element is positioned amidst the functional ones. One may argue that this case could have limited practical interest as, in general, only one defective element does not significantly modify the radiation pattern of the array antenna. However, it may happen that many isolated (i.e., which are surrounded by properly functioning elements) defective elements may be present. Therefore, such a case can be considered as the most critical scenario against which diagnostic methods have to be checked.

According to the previous discussion, we just rerun the same example as in Fig. 2 but now a single defective element is located at position 13. The corresponding indicator functions are reported in Fig. 3. By looking at such a figure it is evident that the proposed approach performs much better than the MUSIC method presented in [10]. Indeed, I_r (reported on the left column) succeeds in detecting and locating the defective element as well as all the correctly working ones. Instead, from I (reported on the right column) it is even more difficult to detect the defective element since the indicator in correspondence of the faulty elements does not even exhibit a local minimum.

As a final example, we consider the effect of reducing the measurement aperture. This is an important issue since reducing the measurement aperture entails reducing the number of measurements and hence speeding up the overall diagnostic procedure. The corresponding I_r functions are reported in Fig. 4 for the case $MA = [−10λ, 10λ]$ and $[−7λ, 7λ]$,

respectively, while the array is kept the same as for previous examples. In particular, for these cases the number of measurements (still taken with a $\lambda/2$ step) are $M = 41$ and $M = 29$ and the SNR has been fixed at $20 dB$. As can be seen, the defective element is still clearly detected. This confirms the weak dependence of MUSIC performances on the measurement aperture. In particular, it is interesting to remark that the proposed method works well also for the case reported on the right panel of such a figure, where the dimension of the noise subspace is only 3. This is of course consistent with MUSIC theory which prescribes that $M \geq N+1$. The latter condition can be considered as a prescription of how large the measurement aperture must be once the array to be diagnosed has been given. In particular, for the case at hand, having chosen a sampling step of $\lambda/2$, the measurement aperture should be at least 13.5λ in size. Note that we just considered MA of 14λ.

V. CONCLUSION

In this contribution we considered the problem of detecting turned off defective elements which can be located inside an array antenna from near-field measurements. In particular, we focused on the MUSIC based method which has recently been proposed in [10].

First, we showed that the MUSIC presented in [10] is in general no better than BTM or MM. This is because the correlation matrix R is rank deficient, which makes the signal subspace of dimension one, regardless of the number of elements in the array. Then, to cope with this limitation, here we proposed a simple scheme for recovering the rank of R based on a suitable arrangement of data in terms of a Toeplitz matrix. In particular, this was possible after casting the problem in the spatial frequency domain. Numerical simulations actually showed that the proposed method outperforms the MUSIC implementation presented in [10]. In particular, the method works well also for a limited measurement aperture as long as $M \geq N + 1$ and the field is sampled at $\lambda/2$.

Of course the considered 2D scalar case is a rather simple scenario and should be meant as a way to more easily convey the discussion and show the numerical examples. However, the study can be easily extended to more realistic scenarios and this is actually one of our commitments for future developments.

REFERENCES

[1] J. J. Lee, E. M. Ferren, D. P. Woollen, and K. M. Lee, "Near-field probe used as a diagnostic tool to locate defective elements in an array antenna," *IEEE Trans. Antennas Propag.*, vol. AP-36, no. 6, pp. 884–889, Jun. 1988.

[2] L. Gattoufi, D. Picard, D. Rekiouak, and J. C. Bolomey, "Matrix method for near-field diagnostic techniques of phased arrays," in *Proc. IEEE Int. Symp. Phased Array Syst. Technol.*, Oct. 1996, pp. 52–57.

[3] B.-K. Yeo and Y. Lu, "Array failure correction with a genetic algorithm," *IEEE Trans. Antennas Propag.*, vol. 47, no. 5, pp. 823–828, May 1999.

[4] J. A. Rodriguez, F. Ares, H. Palacios, and J. Vassallo, "Finding defective elements in planar arrays using genetic algorithms," *Prog. Electromagn. Res.*, vol. 29, pp. 25–37, 2000.

[5] A. Patnaik, B. Chowdhury, P. Pradhan, R. K. Mishra, and C. Christodolou, "An ANN application for fault finding in antenna arrays," *IEEE Trans. Antennas Propag.*, vol. 55, no. 3, pp. 775–777, Mar. 2007.

[6] A. Patnaik, B. Chowdhury, P. Pradhan, R. K. Mishra, and C. Christodolou, "Rapid method for finding faulty elements in antenna arrays using far field pattern samples," *IEEE Trans. Antennas Propag.*, vol. 57, no. 6, pp. 1679–1683, Jun. 2009.

[7] O. M. Bucci, M. D. Migliore, G. Panariello, and P. Sgambato, "Accurate diagnosis of conformal arrays from near-field data using the matrix method," *IEEE Trans. Antennas Propag.*, vol. 53, no. 3, pp. 1114–1120, Mar. 2005.

[8] M. Bertero and P. Boccacci, *Introduction to Inverse Problems Imaging*. Boca Raton, FL, USA: CRC Press, 1998.

[9] A. Buonanno and M. D'Urso, "Large phased arrays diagnostic via distributional approach," *Prog. Electromagn. Res.*, vol. 92, pp. 153–166, 2009.

[10] A. Buonanno and M. D'Urso, "A novel strategy for the diagnosis of arbitrary geometries large arrays," *IEEE Trans. Antennas Propag.*, vol. 60, no. 2, pp. 880–885, Feb. 2012.

[11] A. Dell'Aversano, A. Natale, and R. Solimene, "Comparison between different decorrelation techniques in vital sign detection," *Adv. Electromagn.*, vol. 5, no. 2, pp. 53–58, 2016.

[12] R. O. Schmidt, "Multiple emitter location and signal parameter estimation," *IEEE Trans. Antennas Propag.*, vol. AP-34, no. 3, pp. 276–280, Mar. 1986.

[13] T.-J. Shan, M. Wax, and T. Kailath, "On spatial smoothing for direction-of-arrival estimation of coherent signals," *IEEE Trans. Acoust., Speech Signal Process.*, vol. ASSP-33, no. 4, pp. 806–811, Aug. 1985.

[14] R. Solimene and A. Cuccaro, "Back-propagation imaging by exploiting multipath from point scatterers," *Inverse Problems*, vol. 33, no. 10, 2017, Art. no. 105010.

[15] R. Solimene, A. Brancaccio, J. Romano, and R. Pierri, "Localizing thin metallic cylinders by a 2.5-D linear distributional approach: Experimental results," *IEEE Trans. Antennas Propag.*, vol. 56, no. 8, pp. 2630–2637, Aug. 2008.

[16] R. Solimene, I. Catapano, G. Gennarelli, A. Cuccaro, A. Dell'Aversano, and F. Soldovieri, "SAR imaging algorithms and some unconventional applications: A unified mathematical overview," *IEEE Signal Process. Mag.*, vol. 31, no. 4, pp. 90–98, Jul. 2014.

[17] R. Solimene, G. Ruvio, A. Dell'Aversano, A. Cuccaro, M. J. Ammann, and R. Pierri, "Detecting point-like sources of unknown frequency spectra," *Prog. Electromagn. Res. B*, vol. 50, pp. 347–364, 2013.

[18] S. U. Pillai and Y. Lee, "Coherent signal classification using symmetry considerations," *IEEE Trans. Acoust., Speech Signal Process.*, vol. 37, no. 1, pp. 135–138, Jan. 1989.

[19] S. U. Pillai and B. H. Kwon, "Forward/backward spatial smoothing techniques for coherent signal identification," *IEEE Trans. Acoust., Speech, Signal Process.*, vol. 37, no. 1, pp. 8–15, Jan. 1989.
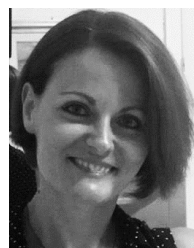
ANGELA DELL'AVERSANO received the Laurea degree *(summa cum laude)* in electronic engineering from the Seconda Università di Napoli (SUN), Aversa, Italy, in 2012, and the Ph.D. degree in electronic engineering, in 2014. Then, she joined the SUN Research Group in applied electromagnetic fields. She is currently a Project Engineer with B&B srl. Her main research interests include inverse scattering problems and microwave imaging.

ANDREA NATALE received the Laurea degree *(summa cum laude)* and the Ph.D. degree in electronic engineering from the Seconda Università di Napoli (SUN), Aversa, Italy, in 2014 and 2017, respectively. His main research interests include inverse scattering problems and microwave imaging via spectral methods.

ANTONIO CUCCARO received the Laurea degree *(summa cum laude)* in electronic engineering from the Seconda Università di Napoli, Aversa (SUN), Italy, in 2012, and the Ph.D. degree in electronic engineering, in 2015. He then joined the Research Group in applied electromagnetic fields of SUN. Then he was Research Fellow with the University of Campania. He is currently a Project Engineer with B&B srl. His main fields of interest are through-the-wall imaging applications, biomedical imaging, antenna design and diagnostics.

RAFFAELE SOLIMENE (SM'19) received the Laurea degree *(summa cum laude)* and the Ph.D. degree in electronic engineering from the Seconda Università di Napoli (SUN), Aversa, Italy, in 1999 and 2003, respectively. In 2002, he became an Assistant Professor with the Faculty of Engineering, University Mediterranea of Reggio Calabria, Italy. Since 2006, he has been with the Dipartimento di Ingegneria, University of Campania Luigi Vanvitelli, where he is currently an Associate Professor. His research activities focus on inverse electromagnetic problems with applications to inverse source and array diagnostics, non-destructive subsurface investigations, through-the-wall and GPR imaging, breast cancer detection. On these topics, he coauthored more than 200 scientific works and organized several scientific sessions.

● ● ●